Noncanonical Adult Human Neurogenesis and Axonal Growth as Possible Structural Basis of Recovery From Traumatic Vegetative State

Clinical Medicine Insights: Case Reports
Volume 10: 1–10
© The Author(s) 2017
Reprints and permissions:
sagepub.co.uk/journalsPermissions.nav
DOI: 10.1177/1179547617732040

Yulia Vainshenker[1], Vsevolod Zinserling[2,3], Alexander Korotkov[1] and Svyatoslav Medvedev[1]

[1]N.P. Bechtereva Institute of the Human Brain of the Russian Academy of Sciences (IHB RAS), Saint Petersburg, Russia. [2]Department of Pathology, Saint Petersburg State University, Saint Petersburg, Russia. [3]Department of Pathology, S.P. Botkin Clinical Infectious Diseases Hospital, Saint Petersburg, Russia.

ABSTRACT: Patient recovering from traumatic vegetative state has suddenly died from cardiac arrest. In-life improvement of consciousness appeared after reduction of generalized spasticity due to botulinum toxin administration. Neuropathologic examination revealed Musashi1+, Nestin+, PCNA+, and Ki67+ cells in the hippocampus, frontal, parietal and occipital cortex, caudate, thalamus, mammillary bodies, brainstem, cerebellum, and near the posterior horn of the lateral ventricle. New neurons with neurite growth (TUC4+) appeared in corpus callosum. At the same time, axonal growth was detected in all areas of interest. New cells whose functional state was continuously improving, as revealed by in-life neurologic and positron emission tomography monitoring, have mainly been found in brain areas without neuropathologic signs of damage. We suggest that the possible role of neurogenesis consists in improvement of the microenvironment and interneuron interactions, whereas the activation of neurogenesis and the induction of neurite growth may be associated with reduction of spasticity.

KEYWORDS: adult human neurogenesis, axonal growth, functional state of the brain, vegetative state, improvement of consciousness, botulinum toxin therapy of spasticity

RECEIVED: May 18, 2017. **ACCEPTED:** July 28, 2017.

PEER REVIEW: Four peer reviewers contributed to the peer review report. Reviewers' reports totaled 596 words, excluding any confidential comments to the academic editor.

TYPE: Case Report

FUNDING: The author(s) disclosed receipt of the following financial support for the research, authorship, and/or publication of this article: Monitoring of the patient was funded by the Program of Presidium of Russian Academy of Sciences "Fundamental Sciences to Medicine." Reagents for IHC were provided by Merz Pharmaceuticals GmbH, Frankfurt, Germany.

DECLARATION OF CONFLICTING INTERESTS: The author(s) declared no potential conflicts of interest with respect to the research, authorship, and/or publication of this article.

CORRESPONDING AUTHOR: Alexander Korotkov, N.P. Bechtereva Institute of the Human Brain of the Russian Academy of Sciences (IHB RAS), 9 Acad. Pavlova Street, Saint Petersburg 197376, Russia. Email: korotkov@ihb.spb.ru

Introduction

The number of patients with long-lasting disorders of consciousness (vegetative state [VS]/unresponsive wakefulness syndrome and minimal conscious state) after traumatic brain injury (TBI) is increasing.[1] However, the prognosis and treatment of these disorders are not well elaborated. Severe diffuse axonal injury (DAI), according to autopsy and structural imaging data, is often responsible for traumatic disorders of consciousness.[2–4]

Clinical evaluation remains the leading instrument for determining the impairment of consciousness and higher brain functions, whereas neuroimaging studies are essential in the absence of the patient's voluntary behavioral reactions.[1,5,6]

Patterns of activation in the fronto-temporo-parietal cortex according to positron emission tomography (PET) and functional magnetic resonance imaging (MRI) data accurately correspond to the level of awareness and higher brain functions in these patients. However, PET is considered to be more informative in terms of complementing bedside examinations and predicting the long-term recovery of patients with VS.[5–8]

Regarding functional disorders of the brain, with or without structural damage associated with impaired consciousness, it has been suggested that the appearance of behavioral signs of awareness is probably related to the apparent integrity of motor pathways and the restoration of normal patterns of activity in frontal/prefrontal cortical-striatopallidal thalamocortical loop systems.[4,9] However, the mechanisms of this recovery remain unexplored.

It is assumed that in addition to functional changes, structural changes may play a key role in the restoration of consciousness,[1,9] and anatomically different forms of axonal growth[10] may participate in the recovery of interneuronal connections and interactions in the central nervous system[9,11] and may be modulated.[12] The existence of adult neurogenesis and its capacity for activation in the presence of various physiologic and pathologic factors (such as damage and neurodegeneration) have been demonstrated in the brains of mammals, including humans. Considering adult neurogenesis as a potential mechanism for the functional repair of the brain, the elicitation of intrinsic and extrinsic conditions in which neurogenesis is activated and new cells not only survive and mature but also integrate into the neuronal network may have important applied significance for the development of treatment programs.[13–16]

The aim of this work was to compare the morphologic changes in the brain with the results of neurologic and PET monitoring, which reflects the restoration of consciousness and improvements in the functional state of the brain.

Materials and methods

Longitudinal case report

A 39-year-old woman was admitted to our clinic for the first time in a traumatic VS, whose duration at that time was 5 months. The cause of initial brain damage was severe TBI with skull fracture, DAI II[2] with contusion in the polar parts of the left temporal and frontal lobes, and subarachnoid hemorrhage. Fractures of the ribs and left shank were detected in the acute period of trauma. In-life monitoring and treatment lasted for 13 months and included 2 hospitalizations at the clinic (lasting 1 month each), with an interval of 7 months between them. During both hospitalizations to treat spasticity,[17–19] botulinum toxin (BT) A (incobotulinumtoxinA; Merz Pharma GmbH & Co. KGaA, Frankfurt, Germany) was injected into all spastic muscles[17,18]; the total dose was 800 U (20 U/kg of body mass) at the first hospitalization and 300 U at the second. In addition, after the first hospitalization, the patient began to receive an *N*-methyl-D-aspartate receptor (NMDA) receptor antagonist (memantine) and a carbonic anhydrase inhibitor (acetazolamide). Because of repeated infection (pneumonia), the patient received courses of antibacterial therapy 3 times. At both hospitalizations, clinical neurologic examinations (the level of consciousness was assessed with the Coma Recovery Scale-Revised [CRS-R],[20] and assessment of muscle tone was performed according to the modified Ashworth Scale [MAS][21]) and PET were performed prior to and 3 weeks after treatment. All examinations (including electroencephalography [EEG], MRI and PET) and treatments were conducted according to the medical board's decisions and the protocol approved by the Institutional Academic Council of the N.P. Bechtereva Institute of the Human Brain of the Russian Academy of Sciences (IHB RAS) and the local ethical committee. Written informed consent was obtained from the patient's mother. When not hospitalized, the patient remained at home.

In the months after the second hospitalization, against a background of continuous positive dynamics, the patient (40 years old at that point) died due to sudden cardiac failure. Along with a standard autopsy, a neuropathologic brain analysis was also performed.

PET examination

^{18}F-fluorodeoxyglucose ([18F]FDG) was prepared via the classical nucleophilic fluorination approach using krypofix 2.2.2 as a phase transfer catalyst following alkali hydrolysis.[22,23] Synthesis was fully automated with the aid of a customized general-purpose [18F] nucleophilic fluorination module,[24] providing a high-purity product with a 60% radiochemical yield (not decay corrected).

Positron emission tomography data acquisition was performed with a PC2048-15B camera (Scanditronix, Uppsala, Sweden) with an in-plane spatial resolution of 6.5 mm full width at half maximum (FWHM) in the center of the field of view (matrix = 128 × 128, 15 slices, voxel size = 2 mm × 2 mm × 2 mm, 15 parallel slices, interslice distance of 6.5 mm).

To minimize head movements, the patient's head was placed in a plastic head mold, and straps were placed around the chin and the forehead.

^{18}F-fluorodeoxyglucose was injected intravenously at a mean dose of 185 MBq. The emission measurement was recorded in static 2-dimensional acquisition mode. Acquisition began 30 minutes after bolus injection of [18F]FDG; 2 15-minute frames were obtained and reconstructed. Images were converted into Analyze format using MRIcro (http://www.cabiatl.com/mricro).

Positron emission tomography image preprocessing was performed with Statistical Parametric Mapping software (SPM 12; Wellcome Department of Cognitive Neurology, London, UK; http://www.fil.ion.ucl.ac.uk/spm) implemented in MATLAB 7.6 (MathWorks Inc., Sherborn, MA, USA), which included spatial normalization to the MNI space and smoothing with a 13-mm FWHM Gaussian filter. The 2 images from each PET study were averaged with the Imcalc SPM add-on and used for further analysis.

A nonparametric voxelwise simple linear regression with the scan time as a predictor and the normalized cerebral metabolic rate of glucose (nCMRGlc) as variables was performed using the Statistical nonParametric Mapping (SnPM) toolbox.[25] Single-subject simple correlation with a single covariate of interest (vector −1.5 −0.5 0.5 1.5) was performed to test the hypothesis that the patient's nCMRGlc increased during the course of monitoring. The SnPM tests were performed based on 24 permutations of the sample data (maximum for 4 scans that we have). Positive correlations were assessed using $P < .05$, uncorrected for multiple tests, as a cut-off for statistical significance.

Identification of the anatomical localization of areas with increased glucose metabolism uptake over time was performed with XjView toolbox (http://www.alivelearn.net/xjview8/).

Neuropathologic examination

During autopsy, the brain was retrieved, and after 1 month of fixation in a puffer formalin solution, it was studied macroscopically in a series of frontal slices. Thirty-two slices in marked paraffin blocks were used for histologic evaluation (Leica HC microscope; Leica Microsystems, Buffalo Grove, IL, USA). Special attention was paid to the brain areas in which functional restoration was observed according to the data of topical neurologic diagnostics and PET. The paraffin slices were prepared according to standard techniques and stained with hematoxylin-eosin. Microscopically, sites of gliosis in the investigated samples of brain tissue were not detected.

To detect neural stem and progenitor cells (NSPCs), rabbit monoclonal anti-Nestin antibody clone SP103 (Spring Bioscience; Cat# SPB-M4034, RRID:AB_2631206) and a rabbit polyclonal antibody against the Musashi1 RNA-binding

protein (MyBioSource; Cat#MBS611647, RRID:AB_2631207) were used. To detect proliferating cells, a rabbit polyclonal antibody against proliferating cell nuclear antigen (PCNA) (Diagnostics-BioSystems; Cat#RP125-05, RRID:AB_2631208) and monoclonal mouse anti-human Ki67 antigen clone MIB-1 (Dako; Cat# M724001-2, RRID:AB_2631211) were used. To detect postmitotic neurons with the initiation of neurite outgrowth, we used a rabbit polyclonal antibody against the TUC-4 protein (Millipore; Cat# AB5454, RRID:AB_91876). To detect the mature differentiated/postmitotic neural cells, a rabbit polyclonal antibody against NeuN (Millipore; Cat# ABN78, RRID:AB_10807945) was used. Immunohistochemical (IHC) analyses were performed according to the manufacturer's recommendations.

As a positive control, we used the brains of 2 fetuses (1 man and 1 woman, spontaneous abortions at 24-26 weeks of gestation). As a negative control, the brain of a 46-year-old male adult who died from sudden cardiac death without clinical or morphologic signs of brain damage was used. The localization of tissue retrieval in the adult was similar to that in the patient. In the fetuses, tissue was retrieved from the periventricular area. The reaction was visualized via standard techniques (horseradish peroxidase, diaminobenzidine). If the dye was found in one or more cells within the investigated fields of view (preparations from one sample/slice of a brain, slice thickness: 3 µm), the result was considered positive for every IHC marker. The number of cells was estimated in field of view with ×20 field lens (0.561 mm^2).

Results

Dynamics of neurologic symptoms

The initial status (before the first course of BT therapy) was recorded as follows. The patient sleeps; eyes open after pain stimulation, not reacting to the surrounding environment; sometimes yawns; salivation occurs. Visual and acoustic startle reflexes are absent. Vertical and horizontal passing gaze divergence (more often to the left) and loss of conjugate ocular movement are observed. Corneal reflexes are present, symptoms of oral automatism with an exaggerated reflex region, decorticate posture with a generalized increase in muscle tone up to 4 scores MAS, laterocollis and "striate finger" of the right foot, deep reflexes from the extremities are reinforced symmetrically with bilateral top and bottom flexor symptoms of Rossolimo. Postural-tonic reactions (spontaneous and pain induced) were observed. There were chronic tracheostoma and gastrostoma.

After the first BT course, muscle tone considerably decreased, remaining conserved only in the muscles of the distal parts of the extremities (1 MAS score). By the second hospitalization (7 months later), tone had increased 1 to 2 points on the MAS, but after a course of BT, it again decreased to physiologic levels (0 point on the MAS). Signs of dystonia and postural-tonic reactions regressed after the first course of BT and did not occur again.

With the decrease in muscle hypertonicity, the level of consciousness improved: for the first hospitalization, from 3 to 10 points (a gain of 7 points) CRS-R, and for the second hospitalization, from 13 to 18 points (a gain of 5 points). For the 7 months between hospitalizations, the gain was 3 points CRS-R, but improvement was observed prior to the recurrent increase in muscle tone.

Signs of restoration of motor, visual, and acoustical reactivity as well as pain comprehension occurred immediately after the first course of BT and accrued further. Locomotion in the extremities initially appeared in the form of the localization of pain stimuli and seizing symptoms and later resembled normal spontaneous movements and repetitive movements in the extremities (more often in a foot) in response to a verbal command. Visual reactions to the surrounding environment gradually appeared, including blink phenomenon, gaze fixation, and visual pursuit. Conjugate eye movements and rotation of the eyes, head, and neck toward a visual stimulus or the sound of a personally meaningful object gradually appeared.

By the second hospitalization, signs of emotional experience and recollections, displayed in situation-driven mimic reactions, were observed. A grimace of displeasure, sometimes with motor excitation, was observed if her husband said he was leaving. After the second course of BT, in a similar situation after the husband left, the patient turned away, displaying a total unwillingness to reestablish contact. At this time, the resist eye-opening phenomenon was recorded. In addition, the patient began to visually identify some acquaintances, showing distinct emotional reactions corresponding to memories of these people.

The patient remained sleepy, and despite some positive dynamics in the span of wakefulness, did not exhibit articulated movements or speech. Control of pelvic functions was also absent.

During the period of monitoring, a reduction in the reflex regions of the symptoms of oral automatism and the appearance of laryngeal reflex and swallowing was observed. In addition, salivation stopped, pyramidal symptoms were changed, and pathologic plantar responses regressed. Neither seizures nor epileptic EEG activity during monitoring was registered.

Thus, restoration of consciousness to a "minimal conscious state plus"[7] was observed in this VS patient. According to the topical neurologic diagnosis,[26] the following areas of the brain participated in maintenance of the reduced motor, visual, oculomotor, and acoustical reactivity of the patient: frontal lobes of hemispheres, anterior subcortical nuclei, temporal associative cortex of the left hemisphere (the patient is right-handed), occipital cortex, pons, midbrain, and connections with the cerebellum. The ability to localize pain stimuli reflects the restoration of structures of the lateral nociceptive system (somatosensory cortex, anterior subcortical nuclei, and thalamus). The appearance of signs of emotional experience and memory tied to the identification and recollection of objects showed improvement of the functions of the limbic system and

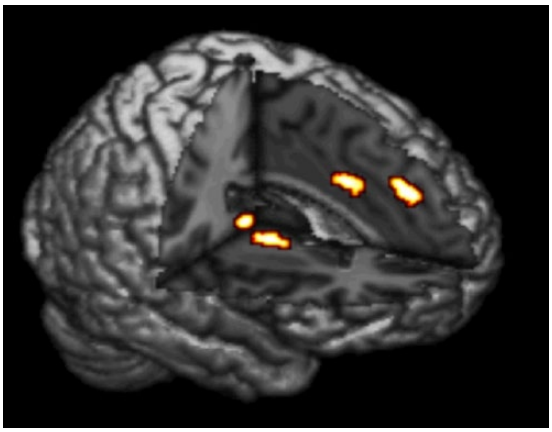

Figure 1. Areas of increase in glucose metabolism during the course of monitoring.

hippocampus. The appearance of selectivity of symptoms of oral automatism, normal reflexes, and frontal phenomena may be viewed as restoration of the function of the cortex of both hemispheres.

Results of PET monitoring

The dynamics of glucose metabolism according to PET are presented in Figure 1 and Table 1.

Thus, during PET monitoring, an increase in glucose metabolism was found in the frontal, temporal, and occipital lobes; the anterior subcortical nuclei of both hemispheres; and the thalami, brainstem, and cerebellum.

Results of neuropathologic examination

Macroscopically, the brain of our patient appeared unchanged with the exception of a posttraumatic brownish area due to the deposition of hemosiderin at the pole of the left temporal lobe and, more moderately, in the neighboring basal parts of the left lobar lobe (Figure 2). Microscopically, fields of gliosis were not detected in other brain regions.

Results of IHC study of samples of the patient's brain are presented in Table 2 and Figures 3 and 4.

The number of NSPCs revealed using any single IHC marker in the studied samples was small (from 1 to 3 in the field of view, 0.561 mm^2). The maximum number (3 cells Musashi1$^+$) was observed in a sample collected from the anterior cingulate cortex. The number of proliferating cells was also small (1-3 cells), except in the sample taken from the midbrain, in which approximately 20 Ki67$^+$ cells were detected (Figure 3).

TUC4$^+$ cells were found in all studied brain samples, along with staining of cell bodies (nucleus and/or cytoplasm); in some samples, staining of the axon was observed as well. The number of TUC4$^+$ cells was small. The maximum number of cells (up to 5) was observed in most of fields of view under a ×20 objective (0.561 mm^2) in the samples taken from the right anterior cingulate cortex, the right temporal lobe, the area adjacent to the posterior horn of the left lateral ventricle, and the corpus callosum (up to 12) (Figure 4A-D).

In slices from the corpus callosum, the accumulation of nuclei of nondifferentiated cells was also detected in the slices stained with hematoxylin-eosin (Figure 4E-F).

In the positive control (fetuses), against a background of a significant number of cells with roundish nuclei in the wide subependimal zone, clear positive staining of cells by all tested serum samples was observed (Figure 5). In the negative control, NeuN$^+$ cells were found in all investigated areas but not in the corpus callosum. The other IHC markers were negative.

Thus, the IHC evaluation revealed the presence of NSPCs (Musashi1$^+$ and/or Nestin$^+$) in the frontal, parietal, and occipital lobes and the caudate of both hemispheres as well as the left hippocampus, the subependymal zone of the left thalamus and the area near the border of the posterior horn of the left lateral ventricle and the mammillary bodies, pons, right cerebellar hemisphere, and vermis.

Both PCNA$^+$ and Ki67$^+$ cells were observed in the left hippocampus. PCNA$^+$ cells were found in the left postcentral gyrus and the left occipital lobe, left thalamus, right caudate, and mammillary bodies. Ki67$^+$ cells were found in the area near the border of the posterior horn of the left lateral ventricle in the left half of the midbrain. TUC4$^+$ cells were revealed in all investigated samples, including those in which Musashi1$^+$, Nestin$^+$, PCNA$^+$, and Ki67$^+$ cells were not found. In the corpus callosum, only TUC4$^+$ cellular bodies were observed in the absence of other IHC$^+$ cells including NeuN$^+$ cells.

Discussion

Our data demonstrated the presence of NSPCs, proliferating cells, and new neurons and evidenced the presence of neurogenesis and increase in glucose utilization in a number of areas of the brain of a 40-year-old patient recovering from a traumatic VS.

According to data in the literature, in adult patients who die without brain damage, NSPCs are absent outside of zones of neurogenesis.[14] The absolute number of new cells in primary neurogenic zones is small, and these cells were not always found using IHC markers.[14,15] The results of our negative control histologic analysis corresponded to these findings and showed only NeuN$^+$ neural cells.

Most of the available data on the presence and activation of neurogenesis in canonical neurogenic and nonneurogenic brain areas have been obtained in animal experiments. Singular studies of samples of human brains obtained during operative interventions or autopsy in patients after TBI, stroke, or hypoxic-ischemic encephalopathy are limited by canonical neurogenic areas and, less often, by the region of obvious structural-functional damage.[13–16] We could not find any reports of adult neurogenesis in various brain areas recovering their activity during the restoration of consciousness.

The presence of Musashi1$^+$ and Nestin$^+$ cells in the left hippocampus (unilateral to structural contusional brain damage)

Table 1. Areas of increase in glucose metabolism during the course of monitoring.

NO.	LOCALIZATION	CLASTER SIZE, VOXELS	PSEUDO *T*	LOCAL MAXIMA, MM
1	R Cerebellum R Parahippocampal G (BA 35) Midbrain Brainstem Vermis R Insula L Fusiform gyrus (BA 37) R Hippocampus R Inferior frontal G (BA 47) R Thalamus R Amygdala Mammillary body	6339	6.3884	40 8 –18
2	R Middle frontal G (BA 6) R Superior frontal G (BA 8, 9)	369	5.0656	28 16 48
3	L Middle occipital gyrus (BA 18, 19)	259	4.8644	–30 –86 10
4	L Middle frontal gyrus (BA 6) L Medial frontal gyrus (BA 8) L Cingulate gyrus (BA 24, 32)	595	4.7968	–22 14 50
5	L Postcentral (BA 2, 3) L Precentral G (BA 4) L Inferior parietal lobule (BA 40)	139	4.3451	–42 –20 44
6	L Inferior parietal lobule (BA 40) L Supramarginal G (BA 40)	141	4.2475	–50 –36 36
7	L Inferior temporal gyrus BA (20) Fusiform gyrus (BA 37) L Middle temporal gyrus (BA 21) L Parahippocampal gyrus L Hippocampus L Amygdala L Superior temporal gyrus (BA 42) L Globus pallidus	596	4.0416	–54 –20 –22
8	R Inferior occipital G (BA 19) R Fusiform gyrus G (BA 37)	340	3.9758	30 –88 –2
9	L Precentral_L (aal) (BA 4) L Inferior frontal gyrus (BA 44, 45) L Middle frontal G (BA 6)	201	3.8313	–48 2 26
10	L Superior temporal gyrus (BA 41) L Insula L Middle temporal gyrus (BA 22) L Angular G (BA 39) L Supramarginal L (BA 40)	464	3.8278	–40 –34 12
11	L Precuneus (BA 7) L Paracentral lobule L (BA 5)	222	3.7712	–8 –40 42
12	L Middle frontal gyrus (BA 10)	125	3.2395	–24 44 22
13	L Cerebellum	62	2.8013	–42 –52 –40
14	L Cingulate (BA 24, 31)	13	2.7199	–10 –10 46
15	R Inferior frontal G (BA 45) R Insula	104	2.7113	40 22 16
16	R Medial frontal G (BA 10, 11) R Anterior vingulate G (BA 32)	106	2.6003	10 44 –6
17	L Angular G (BA 39)	41	2.5802	–34 –66 32

Abbreviations: BA, Brodmann area; R or L, right or left hemisphere.

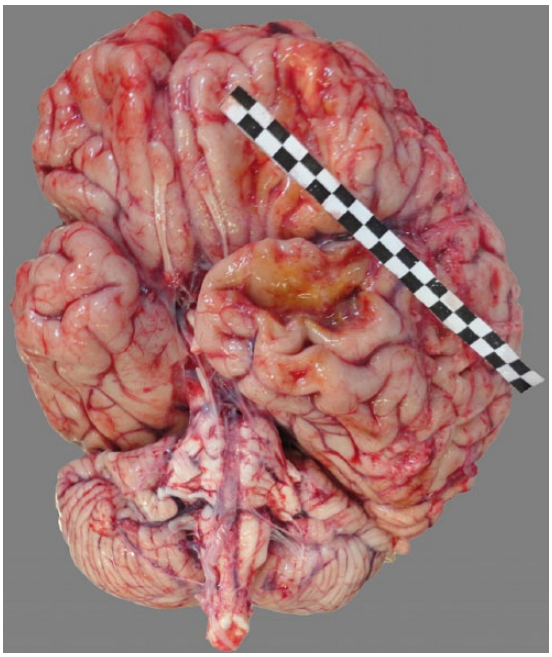

Figure 2. Brain immediately after the autopsy. The brain appeared unchanged with the exception of a posttraumatic brownish area due to the deposition of hemosiderin at the pole of the left temporal lobe and, more moderately, in the neighboring basal parts of the left lobar lobe.

indicates the activation of canonical neurogenesis in the neurogenic brain area.[14] However, the mechanism responsible for the appearance of NSPCs in nonneurogenic areas, as a result of "canonical" migration from neurogenic areas or through initial origination in situ, remains unclear.[16] The further fate of NSPCs also remains unknown; however, the presence of PCNA$^+$ and Ki67$^+$ cells in numerous brain regions (predominantly in the left, damaged hemisphere) may indicate that these cells preserve proliferation activity.[14]

According to experimental data, TUC4$^+$ cells can be either mature or young postmitotic neurons in a maturing stage.[27] In this context, the reason that TUC4$^+$ cells appear in all studied brain areas remains poorly understood. TUC4$^+$ cells were the only new cells detected in the corpus callosum, which makes it possible to surmise that they appeared there as a result of the migration of new neurons to the frontal lobes[16] or nearby "destinations." Taking into consideration the presence of DAI II in our patient, it is also possible that functional role of these new cells consists in reconstruction of axons of corpus callosum.

From the perspective of restoration of interneuronal communications and interactions in a brain, the discovery of cells with activated neurite growth (potential or already realizing) in all investigated brain areas is certainly a significant finding. However, the most important finding of this study was the detection of Musashi1$^+$, Nestin$^+$, PCNA$^+$, and Ki67$^+$ cells in brain areas whose functional state improved during monitoring according to neurologic and PET data. The functional restoration of these areas is related to the restoration of awareness and higher brain functions, in accordance with the anterior forebrain mesocircuit model with the participation of "posterior" brain areas.[4,9,28]

The obtained data correspond to the hypothesis of a reciprocal effect of function (functionally relevant activity) on neurogenesis, which has been described for hippocampal neurogenesis.[15]

The question of the mechanisms responsible for the restoration of brain functions in VS patients remains open. The obtained data indicate possible participation of neurogenesis in the processes of reparation of the brain, providing restoration of its functions. Considering the small number of NSPCs that reach the damaged areas of the brain (or originate in them), it seems unlikely that "structural" integration into functional neuroanatomical systems or replacement of damaged "old" cells by NSPCs is important. We speculate that one of the leading mechanisms of reparation due to neurogenesis is enrichment of the microenvironment and interneuronal interactions due to the newly formed cells.

It is important to note that during the monitoring of our patient, indicators of possible pathologic processes associated with aberrant neurogenesis, such as seizures or epileptiform EEG activity,[13] were not registered.

The existence of neurogenesis in functionally improving brain areas leads to one additional question: Does neurogenesis always accompany restoration of the functional state of the brain (in areas without structural damage) and consciousness, and what mechanisms are responsible for its activation?

After the first hospitalization (during clinical improvement), our patient began to receive the NMDA receptor antagonist memantine, which activates hippocampal neurogenesis according to experimental studies.[29]

The improvement of the functional state of the brain in our patient was likely related to the termination of pathologic hyperafferentation from all spastic muscles after BT.[17,18] A recent experimental animal study that showed the influence of afferentation on mature motor system spinal connections[12] partially supports this notion. It is possible that there is no causal relationship between BT and neurogenesis. However, improvements in the functional state of the brain in its separate areas, associated with the local activation of metabolic, trophic, and electrochemical processes, can appear after the activation of neurogenesis, which occurs as a functionally mediated effect of the reduction of pathologic hyperafferentation.

Taking into account the available experimental animal studies, it is impossible to exclude the possibility of retrograde axonal transport of catalytically active BT A in brain structures.[30] Thus, modulation of neurotransmission and reduction in the release of mediators of pain and inflammation,[30] as a condition for the activation of neurogenesis as well as the induction of neurite outgrowth,[31] can appear as direct central effects of BT.

Table 2. Results of immunohistochemical study (IHC—paraffin).

NO.	LOCALIZATION OF SAMPLES, HEMISPHERE	NESTIN	MUSASHI1	PCNA	KI67	TUC4	NEUN
1	Corpus callosum	–	–	–	–	+	–
2	Anterior cingulate cortex, R	+	+	–	–	+[a]	+
3	Anterior cingulate cortex, L	+	–	–	–	+	+
4	Lateral cortex of frontal lobe, R	–	+	–	–	+	+
5	Lateral cortex of frontal lobe, L	–	–	–	–	+	+
6	Posterior central gyrus, R	+	–	–	–	NA	+
7	Posterior central gyrus, L	+	–	+	–	NA	+
8	Parietal lobe, R	–	–	–	–	NA	+
9	Parietal lobe, L	–	–	–	–	NA	+
10	Occipital lobe, R	+	+	–	–	NA	+
11	Occipital lobe, L	+	–	+	–	NA	+
12	Area near the border of posterior horn of right lateral ventricle, R	–	–	–	–	NA	+
13	Area near the border of posterior horn of lateral ventricle, L	+	–	–	+	+[a]	+
14	Middle temporal gyrus, R	–	–	–	–	+[a]	+
15	Middle temporal gyrus, L	–	–	–	–	+	+
16	Superior temporal gyrus, R	–	–	–	–	+	+
17	Superior temporal gyrus, L	–	–	–	–	+[a]	+
18	Hippocampus, R	–	–	–	–	NA	+
19	Hippocampus, L	+	+	+	+	NA	+
20	Caudate, R	–	+	+	–	NA	+
21	Caudate, L	+	–	–	–	NA	+
22	Thalamus, R	–	–	–	–	+	+
23	Thalamus, L	+[b]	–	+	–	+	+
24	Mammillary bodies	+	–	+	–	NA	+
25	Midbrain, R	–	–	–	–	+	+
26	Midbrain, L	–	–	–	+	+	+
27	Pons	+	–	–	–	NA	+
28	Medulla oblongata, R	–	–	–	–	NA	+
29	Medulla oblongata, L	–	–	–	–	NA	+
30	Hemisphere of cerebellum, R	+	+	–	–	+[a]	+
31	Hemisphere of cerebellum, L	–	–	–	–	+[a]	+
32	Vermis	+	–	–	–	+	+

Abbreviations: NA, not assessed; PCNA, proliferating cell nuclear antigen; R or L, right or left hemisphere.
+indicates cells detected; – indicates not detected.
[a]Visible neurite outgrowth.
[b]Nestin+cell located in the subependymal zone of the left thalamus.

To conclude, our data provide the first evidence of the presence of neurogenesis in functionally recovering areas of the brain, which underlies the restoration of consciousness and the highest brain functions of the adult human brain and

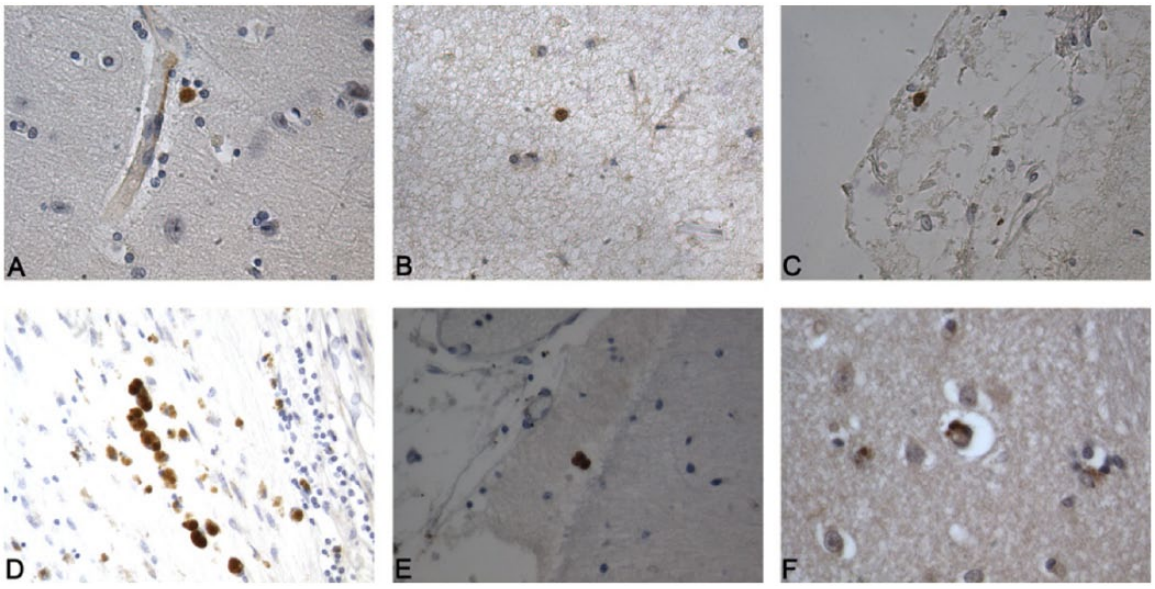

Figure 3. Neural stem and progenitor cells and proliferating cells in "noncanonical" neurogenic brain areas (IHC—paraffin). IHC+ cells are colored brown. (A) Nestin+ cell located in the left anterior cingulate cortex (original magnification ×320). (B) PCNA+ cell located in the left posterior central gyrus (original magnification ×320). (C) PCNA+ cell located in the left occipital lobe (original magnification ×320). (D) Ki67+ cells located in the left half of midbrain (original magnification ×320). (E) Nestin+ cell located in the right hemisphere of cerebellum (original magnification ×320). (F) Mus1+ cell located in the right caudate (original magnification ×640). IHC indicates immunohistochemistry; PCNA, proliferating cell nuclear antigen.

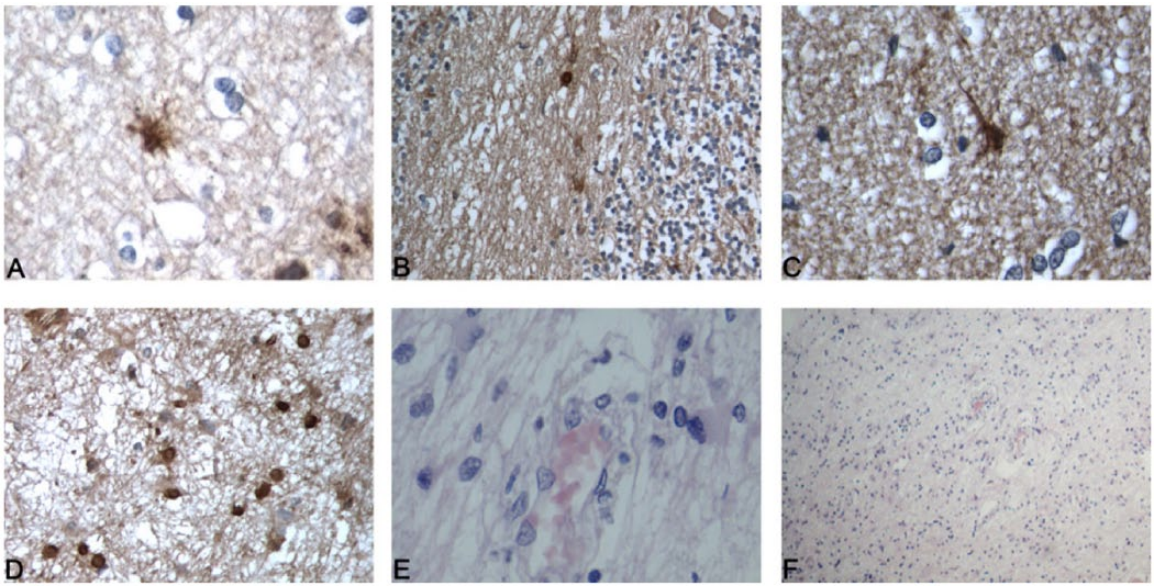

Figure 4. Postmitotic neurons with initiation of neurite growth (IHC—paraffin). TUC4+ cells are colored brown. (A) TUC4+ cells with visible neurite outgrowths located in the right temporal lobe (original magnification ×640). (B) TUC4+ cells with visible neurite outgrowths located in the right hemisphere of cerebellum (original magnification ×250). (C) TUC4+ cell with visible neurite outgrowth located in the area adjacent to the posterior horn of the left lateral ventricle (original magnification ×640). (D) TUC4+ cells located in the corpus callosum (original magnification ×320). (E) hypercellularity in the corpus callosum (hematoxylin-eosin, original magnification ×640). (F) hypercellularity in the corpus callosum (hematoxylin-eosin, original magnification ×100). IHC indicates immunohistochemistry.

the activation of axonal growth. We speculate that one of the leading mechanisms of repair through neurogenesis is enrichment of the microenvironment and interneuronal interactions due to newly formed cells, whereas biological processes accompanying functional restoration may follow the activation of neurogenesis, especially in noncanonical neurogenic brain areas. Future human postmortem IHC studies when compared with in-life clinical data may significantly contribute the understanding of mechanisms of brain restoration.

Limitations of the study

Insurmountable peculiarities of the design of our study prevent us from conclusions about possible cause of appearance of new

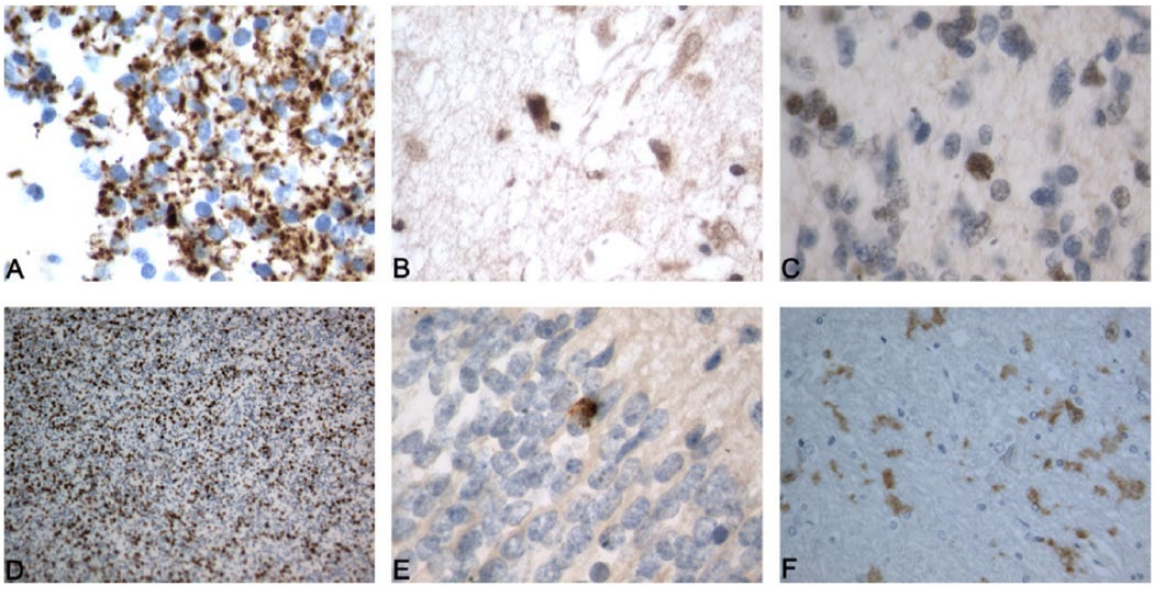

Figure 5. Positive control, light microscopical view of IHC+ cells of the periventricular area of the brain of fetuses (IHC—paraffin). IHC+ cells are colored brown. (A) Nestin+ cells (original magnification ×640). (B) Mus1+ cells (original magnification ×400). (C) PCNA+ cells (original magnification ×640). (D) Ki67+ cells (original magnification ×100). (E) Tuc+ cell (original magnification ×640). (F) NeuN+ cells (original magnification ×250). IHC indicates immunohistochemistry; PCNA, proliferating cell nuclear antigen.

cells and axonal growth (primary damage of the brain or correction of generalized spasticity and muscle pain or medications received by patient or combination of these reasons. Co-labeling analyses would help to define the identity of detected NSPCs and proliferating cells. Further studies are required to clarify these questions.

Acknowledgements

The authors thank Natalia Semenova for assistance in IHC study.

Author Contributions

SM conceived and designed the experiments. YV, VZ, and AK analyzed the data. YV and AK wrote the first draft of the manuscript. SM and VZ contributed to the writing of the manuscript and made critical revisions and approved final version. YV, VZ, AK, and SM agree with manuscript results and conclusions. YV, VZ, AK, and SM jointly developed the structure and arguments for the paper. All authors reviewed and approved the final manuscript.

Availability of the Data

The authors declare that all data supporting the findings of this study are available from the corresponding author (A.K.) on request.

Disclosure and Ethics

The authors have read and confirmed their agreement with the ICMJE authorship and conflict of interest criteria. The authors have also confirmed that this article is unique and not under consideration or published in any other publication. Any disclosures are made in this section.

REFERENCES

1. Dolce G, Sazbon L, ed. *The Post-Traumatic Vegetative State*. Stuttgart, Germany: Thieme; 2002.
2. Adams JH, Jennett B, McLellan DR, Murray LS, Graham DI. The neuropathology of the vegetative state after head injury. *J Clin Pathol*. 1999;52:804–806.
3. Jellinger KA. Neuropathology of prolonged unresponsive wakefulness syndrome after blunt head injury: review of 100 post-mortem cases. *Brain Injury*. 2013;27:917–923. doi:10.3109/02699052.2013.793395.
4. Giacino JT, Fins JJ, Laureys S, Schiff ND. Disorders of consciousness after acquired brain injury: the state of the science. *Nat Rev Neurol*. 2014;10:99–114. doi:10.1038/nrneurol.2013.279.
5. Gosseries O, Di H, Laureys S, Boly M. Measuring consciousness in severely damaged brains. *Annu Rev Neurosci*. 2014;37:457–478. doi:10.1146/annurev-neuro-062012-170339.
6. Stender J, Gosseries O, Bruno M-A, et al. Diagnostic precision of PET imaging and functional MRI in disorders of consciousness: a clinical validation study. *Lancet*. 2014;384:514–522. doi:10.1016/S0140-6736(14)60042-8.
7. Bruno M-A, Majerus S, Boly M, et al. Functional neuroanatomy underlying the clinical subcategorization of minimally conscious state patients. *J Neurol*. 2012;259:1087–1098. doi:10.1007/s00415-011-6303-7.
8. Thibaut A, Bruno MA, Chatelle C, et al. Metabolic activity in external and internal awareness networks in severely brain-damaged patients. *J Rehabil Med*. 2012;44:487–494. doi:10.2340/16501977-0940.
9. Schiff ND. Recovery of consciousness after brain injury: a mesocircuit hypothesis. *Trends Neurosci*. 2010;33:1–9. doi:10.1016/j.tins.2009.11.002.
10. Tuszynski MH, Steward O. Concepts and methods for the study of axonal regeneration in the CNS. *Neuron*. 2012;74:777–791. doi:10.1016/j.neuron.2012.05.006.
11. Oudega M, Perez MA. Corticospinal reorganization after spinal cord injury. *J Physiol*. 2012;590:3647–3663. doi:10.1113/jphysiol.2012.233189.
12. Jiang Y-Q, Zaaimi B, Martin JH. Competition with primary sensory afferents drives remodeling of corticospinal axons in mature spinal motor circuits. *J Neurosci*. 2016;36:193–203. doi:10.1523/jneurosci.3441-15.2016.
13. Kernie SG, Parent JM. Forebrain neurogenesis after focal ischemic and traumatic brain injury. *Neurobiol Dis*. 2010;37:267–274. doi:10.1016/j.nbd.2009.11.002.
14. Sierra A, Encinas JM, Maletic-Savatic M. Adult human neurogenesis: from microscopy to magnetic resonance imaging. *Front Neurosci*. 2011;5:47. doi:10.3389/fnins.2011.00047.
15. Kempermann G. Activity dependency and aging in the regulation of adult neurogenesis. *CSH Perspect Biol*. 2015;7:a018929. doi:10.1101/cshperspect.a018929.
16. Feliciano DM, Bordey A, Bonfanti L. Noncanonical sites of adult neurogenesis in the mammalian brain. *CSH Perspect Biol*. 2015;7:a018846. doi:10.1101/cshperspect.a018846.
17. Vainshenker YI, Ivchenko IM, Korotkov AD, Kataeva GV, Medvedev SV. Polyfunctionality of neurons: the blocking of extreme pathological afferentation

leads to an improvement of the higher functions of the brain. *Hum Physiol*. 2013;39:19–21. doi:10.1134/S0362119713010143.
18. Vainshenker Y, Korotkov A, Melucheva L, Ivchenko I, Medvedev S. Improvement of functional state of the brain as effect of treatment of generalized spasticity with high doses of incobotulinumtoxinA (Xeomin) in patients in a vegetative state. *Toxicon*. 2015;93:S61. doi:10.1016/j.toxicon.2014.11.199.
19. Thibaut A, Chatelle C, Wannez S, et al. Spasticity in disorders of consciousness: a behavioral study. *Eur J Phys Rehab Med*. 2015;51:389–397.
20. Giacino JT, Kalmar K, Whyte J. The JFK Coma Recovery Scale-Revised: measurement characteristics and diagnostic utility. *Arch Phys Med Rehab*. 2004;85:2020–2029.
21. Gregson JM, Leathley M, Moore AP, Sharma AK, Smith TL, Watkins CL. Reliability of the Tone Assessment Scale and the modified Ashworth Scale as clinical tools for assessing poststroke spasticity. *Arch Phys Med Rehab*. 1999;80:1013–1016.
22. Fuchetner F, Steinbach J, Mading P, Johannsen B. Basic hydrolysis of 2-[18F] Fluoro-1,3,4,6-tetra-O-acetyl-d-glucose in the preparation of 2-[18F]Fluoro-2-deoxy-D-glucose. *Appl Radiat Isotopes*. 1996;47:61–66. doi:10.1016/0969-8043(95)00258-8.
23. Gomzina NA, Vassiliev DA, Krasikova RN. Optimization of robotic preparation of 2-[18F]fluoro-2-deoxy-D-glucose based on alkali hydrolysis. *Radiochemistry*. 2002;44:366–372. doi:10.1023/A:1020689314452.
24. Krasikova R. PET radiochemistry automation: state of the art and future trends in 18F-nucleophilic fluorination. *Curr Org Chem*. 2013;17:2097–2107. doi:10.2174/13852728113179990102.
25. Holmes AP, Bair RC, Watson JD, Ford I. Nonparametric analysis of statistic images from functional mapping experiments. *J Cerebr Blood F Met*. 1996;16:7–22. doi:10.1097/00004647-199601000-00002.
26. Duus P. *Topical Diagnosis in Neurology: Anatomy, Physiology, Signs, Symptoms*. 2nd ed. New York: Thieme; 1989.
27. Quinn CC, Chen E, Kinjo TG, et al. TUC-4b, a novel TUC family variant, regulates neurite outgrowth and associates with vesicles in the growth cone. *J Neurosci*. 2003;23:2815–2823.
28. Koch C, Massimini M, Boly M, Tononi G. The neural correlates of consciousness: progress and problems. *Nat Rev Neurosci*. 2016;17:307–321. doi:10.1038/nrn.2016.22.
29. Maekawa M, Namba T, Suzuki E, Yuasa S, Kohsaka S, Uchino S. NMDA receptor antagonist memantine promotes cell proliferation and production of mature granule neurons in the adult hippocampus. *Neurosci Res*. 2009;63:259–266.
30. Matak I, Lacković Z. Botulinum toxin A, brain and pain. *Prog Neurobiol*. 2014;119-120:39-59. doi:10.1016/j.pneurobio.2014.06.001.
31. Coffield JA, Yan X. Neuritogenic actions of botulinum neurotoxin A on cultured motor neurons. *J Pharmacol Exp Ther*. 2009;330:352–358. doi:10.1124/jpet.108.147744.